UNIVERSITY *of York*

This is a repository copy of *A mobile ELF4 delivers circadian temperature information from shoots to roots*.

White Rose Research Online URL for this paper:
https://eprints.whiterose.ac.uk/id/eprint/158324/

Version: Accepted Version

Article:

White Rose
university consortium
Universities of Leeds, Sheffield & York

A mobile ELF4 delivers circadian temperature information from shoots to roots

Wei Wei Chen[1*], Nozomu Takahashi[1*], Yoshito Hirata[2,3], James Ronald[4], Silvana Porco[5], Seth J. Davis[4,6], Dmitri A. Nusinow[7], Steve A. Kay[5,8] and Paloma Mas[1,9,†].

[1]Centre for Research in Agricultural Genomics (CRAG), CSIC-IRTA-UAB-UB, Campus UAB, Bellaterra, 08193 Barcelona, Spain.

[2]Mathematics and Informatics Center, The University of Tokyo, 7-3-1 Hongo, Bunkyo-ku, Tokyo 113-8656, Japan.

[3]Faculty of Engineering, Information and Systems, University of Tsukuba, 1-1-1 Tennodai, Tsukuba, Ibaraki 305-8573, Japan.

[4]Department of Biology, University of York, York, UK.

[5]Keck School of Medicine, University of Southern California, Los Angeles, California 90089, United States.

[6]Key Laboratory of Plant Stress Biology, School of Life Sciences, Henan University, Kaifeng 475004, China.

[7]Donald Danforth Plant Science Center, St. Louis, MO 63132.

[8]Institute of Transformative Bio-Molecules, Nagoya University, Nagoya 464-8601, Japan.

[9]Consejo Superior de Investigaciones Científicas (CSIC), 08028 Barcelona, Spain.

[*]These authors contributed equally the manuscript.

[†]Correspondence to: paloma.mas@cragenomica.es

Abstract

The circadian clock is synchronized by environmental cues, mostly by light and temperature. Elucidating how the plant circadian clock responds to temperature oscillations is crucial to understand plant responsiveness to the environment. Here we found a prevalent temperature-dependent function of the Arabidopsis clock component ELF4 (EARLY FLOWERING 4) in the root clock. Although the root clock is able to run in the absence of shoots, micrografting assays and mathematical analyses show that ELF4 moves from shoots to regulate rhythms in roots. ELF4 movement does not convey photoperiodic information but trafficking is essential to control the period of the root clock in a temperature-dependent manner. At low temperatures, ELF4 mobility is favored, resulting in a slow-paced root clock while high temperatures decrease movement, leading to a faster clock. Hence, the mobile ELF4 delivers temperature information and establishes a shoot-to-root dialogue that sets the pace of the clock in roots.

Introduction

Nearly all photosensitive organisms have evolved timing mechanisms or circadian clocks able to synchronize metabolism, physiology and development in anticipation to the 24-hour light/dark cycles[1]. In *Arabidopsis thaliana*, the molecular clockwork is based on complex regulatory networks of core clock components that generate rhythms in a myriad of biological outputs[2, 3]. Appropriate phasing of biological processes relies on clock resetting by light and temperature cues; a mechanism that requires effective changes in the expression and activity of essential clock components[4]. Circadian clocks are also defined by a conserved feature known as temperature compensation[5]. In contrast to the temperature dependency of many physicochemical and biological activities, the circadian clock is able to maintain a constant period over a range of physiological temperatures. By virtue of different transcriptional, post-transcriptional and post-translational mechanisms[6-9], the plant circadian system buffers the circadian period length. Therefore, the circadian clock is able to sustain a period close to 24-hours within a physiological range of temperatures. An ample collection of light-related factors[10-14] and clock-associated components[9, 15, 16] has been shown to directly or indirectly regulate clock temperature compensation in plants.

Among the Arabidopsis clock components, ELF4 (EARLY FLOWERING 4) was initially identified by its role in photoperiod perception and circadian regulation[17]. Structural and functional studies provided a view of the multiple entry points of ELF4 function within the clock[18]. ELF4 protein assembles into a tripartite complex (Evening Complex, EC) together with ELF3 and LUX ARRHYTHMO or PHYTOCLOCK1 (LUX/PCL1)[19, 20]. The complex regulates

growth and represses circadian gene expression[21, 22]. ELF4 promotes the nuclear localization of ELF3[19] while LUX directly binds to the promoters of the target genes and thus facilitates the recruitment of ELF4 and ELF3[20, 23]. Loss-of-function mutants of any of the EC components lead to arrhythmia[17, 24-26]. Through multiple interactions with light, clock and photomorphogenesis related factors[27], the EC is able to coordinate plant responses to environmental cues including temperature[15, 27-31] although ELF4, ELF3 and LUX also display independent functions from the EC[31-33].

Regarding the circadian structure and organization within the plant, it is broadly accepted that every plant cell harbors a circadian oscillator. However, circadian communication or coupling among cells and tissues varies at different parts of the plant[34-38]. For instance, while cotyledon cells present circadian autonomy[39], different degrees of cell-to-cell coupling have been reported in leaves[40-42], in the vasculature with neighbor mesophyll cells[43], in guard cells[44], in cells at the root tip[45, 46] and within the shoot apex[47]. Long-distance shoot-to-root photosynthetic signaling is also important for clock entrainment in roots[48] and light piping down the root[49] contributes to this entrainment. Micrografting assays and shoot excision[47] suggest the existence of a long-distance mobile circadian signal from shoots to roots. Here we report that ELF4 moves from shoots to control the pace of the root clock in a temperature-dependent manner.

Results

Prevalent function of ELF4 sustaining rhythms in roots

We first approached the investigation of the circadian mobile signal by simultaneously following rhythms in shoots and roots of intact plants[47]. The waveforms of the morning-expressed *CCA1* (*CIRCADIAN CLOCK ASSOCIATED 1*) and *LHY* (*LATE ELONGATED HYPOCOTYL*) promoter activities displayed a long period, slightly reduced amplitude and phase delay in roots (Rt) compared to shoots (Sh) (Fig. 1a-b and Extended Data Fig. 1a). The mRNA rhythmic accumulation assayed by Reverse Transcription-Quantitative Polymerase Chain Reaction (RT-QPCR) followed the same trend (Fig. 1c). Similar patterns were observed for the promoter activity of the evening-expressed clock component *TOC1/PRR1* (*TIMING OF CAB EXPRESSION1/PSEUDO RESPONSE REGULATOR1*) (Extended Data Fig. 1b-c). Therefore, the clock is fully operative in roots but its overall pace is slower and the phase delayed compared to shoots.

Under free-running conditions, the circadian clock is unable to properly run in mutant plants of any of the EC components[17, 24-26]. We therefore examined the role of the EC components in the root clock, and in particular, we focused on ELF4. Circadian time course analyses showed that although some very weak oscillations could be appreciated (Extended Data Fig. 1d), the *CCA1*

103   and *LHY* promoter activities and mRNA expression was suppressed in *elf4-1* mutant compared

104   to WT roots (Fig. 1d and Extended Data Fig. 1e-g) following a similar trend to that described in

105   shoots[22] (Extended Data Fig. 1h-j). Over-expression of ELF4 (ELF4-ox) lengthened the period

106   of *LHY::LUC* (Fig. 1e and Extended Data Fig. 1k) indicating that increased ELF4 activity in

107   roots makes the clock to run slow. The expression of *PRR9 (PSEUDO-RESPONSE*

108   *REGULATOR 9)*, a previously described direct target of the EC in shoots, was clearly up-

109   regulated in *elf4-1* mutant roots (Fig. 1f) suggesting that the EC also represses *PRR9* in roots.

110   Thus, ELF4 plays an important regulatory function in the root clock: mutation compromises

111   rhythms while over-expression lengthens the circadian period.

112

113   RNA-Seq analyses of WT and *elf4-1* mutant roots provided a genome-wide view of ELF4

114   function in roots (Supplementary Table 1). We found that about 15% of the root genes were

115   significantly mis-regulated by the absence of a functional ELF4, with a similar proportion of up-

116   regulated (1297) and down-regulated (1555) genes (Fig. 1g-h and Extended Data Fig. 2a). The

117   expression of core clock genes was amongst the most significantly mis-regulated (Fig. 1i,

118   Extended Data Fig. 2b-i) with a significant fraction of the mis-regulated genes being controlled

119   by the clock, with phase enrichments during the subjective morning and subjective midday (Fig.

120   1j-k). Functional analyses showed that in addition to the enrichment of genes related to the

121   circadian system and rhythmic processes, genes mis-expressed in *elf4-1* mutant were ascribed to

122   several functional categories including among others responses to stimuli (Supplementary Table

123   1). Consistently, mis-expression of ELF4 affected physiological outputs such as the number of

124   lateral roots (Extended Data Fig. 2j). Together, the results indicate a prevalent function for

125   ELF4 sustaining rhythms in roots.

126

127   **ELF4 moves from shoots to regulate oscillator gene expression in roots**

128   Our previous study showed that a signal from shoots is important for circadian rhythms in roots

129   [47]. Micrografting assays are a powerful tool to identify the nature of mobile signals. The grafting

130   technique *per se* does not alter the rhythms in roots[47], as grafted WT scions into WT roots show

131   similar rhythms as non-grafted WT plants (Extended Data Fig. 3a and b). By micrografting

132   different genotypes, we found that grafts of ELF4-ox shoots into *elf4-1* rootstocks [ELF4-

133   ox(Sh)/*elf4-1*(Rt)] (Extended Data Fig. 3c) were particularly efficient in recovering the rhythms

134   in roots (Fig. 2a and Extended Data Fig. 3d). The results are noteworthy as *CCA1::LUC*

135   rhythms are affected in *elf4-1* mutant roots (Fig. 1d). Restoration of the rhythms was reflecting

136   the circadian function exclusively in roots as water instead of luciferin was applied to shoots

137   (ELF4-ox, Sh, H_2O) to avoid luminescence signals leaking from shoots into roots of adjacent

138   wells. Rhythms in roots were also recovered when ELF4-ox scion was grafted into *elf4-2*

139   mutant (Extended Data Fig. 3e) rootstocks (Fig. 2b). To exclude the possibility that the

140 observed results were due to the high over-expression of ELF4-ox plants, we grafted WT shoots

141 into *elf4-1* roots. Although the recovery of the rhythms was not as robust as with ELF4-ox

142 grafts, a rhythmic pattern was observed in roots (Fig. 2c). Thus, ELF4 mRNA or protein are

143 able to move from shoots to roots. This notion was reinforced by the results showing the

144 rhythmic recovery of *elf4-1* rootstocks grafted with ELF4 Minigene (E4MG) scion (Fig. 2d and

145 Extended Data Fig. 3f). These results rule out the possibility that the recovery of the rhythms

146 was just due to the high over-expression of ELF4-ox scion. The influence of shoots as a driving

147 rhythmic force of *elf4-1* rootstocks was also mathematically analyzed with recurrence plots

148 obtained by delay coordinates of the grafting time series. The waveforms of the driving

149 rhythmic force reconstructed from the driven system and their autocorrelation analyses showed

150 a strong periodicity after grafting (Extended Data Fig. 4a-h). In analyses with 10000 randomly

151 shuffled surrogates using as null hypothesis of no serial dependence, we obtained before

152 grafting a p-value of 0.2341 (black dash line) (Extended Data Fig. 4f) and 0.0004 (gray dash

153 line) after grafting (Extended Data Fig. 4h). The statistics are therefore consistent with the

154 notion that rhythms in roots are being forced by a signal from shoots.

155

156 To investigate whether the mRNA could be the mobile signal, we performed RT-QPCR time

157 course analyses of roots from ELF4-ox (Sh)/*elf4-1*(Rt) grafts. Our results showed no detectable

158 amplification of *ELF4* mRNA at any time point analyzed (Fig. 2e), which suggest that *ELF4*

159 mRNA did not move through the graft junctions. To confirm this notion, we injected purified

160 ELF4 protein into *elf4-1* mutant (Extended Data Fig. 5a-c). Injection in shoots was able to

161 restore rhythms in roots (Fig. 2f). The percentage of ELF4-injected plants with recovered

162 rhythms was low (5-8%) but was reproducibly observed in different biological replicates. The

163 fact that rhythms were actually restored (Relative Amplitude Errors, RAE<0.6) is supportive of

164 a mobile ELF4 protein from shoots to roots. Rhythmic recovery was not apparent when purified

165 GFP (GREEN FLUORESCENT PROTEIN) was injected (Fig. 2f). The movement of ELF4

166 protein was further assayed by using shoots of plants over-expressing ELF4 fused to GFP

167 grafted into *elf4-1* mutant roots. Confocal imaging showed that ELF4-GFP fluorescent signals

168 accumulated in the vasculature of *elf4-1* mutant rootstock, across the graft junctions (Fig. 2g-h

169 and Extended Data Fig. 5d-e). Furthermore, Western-blot analyses of roots from ELF4-GFP

170 (Sh)/*elf4-1*(Rt) micrografts showed that ELF4 protein was effectively detected as a band of the

171 expected size (arrows in Fig. 2i) not present in protein extracts of *elf4-1* mutant roots (Fig. 2i).

172 Grafting ELF4-ox fused to three GFPs (ELF4-x3GFP) scion into *elf4-2* mutant rootstock did not

173 lead to an obvious recovery of rhythms (Fig. 2j and Extended Data Fig. 5f) suggesting the

174 requirement of a mobile ELF4 protein. The ELF4-x3GFP is still functional as its over-

175 expression in the *elf4-1* mutant background restored the hypocotyl phenotypes of *elf4-1* mutant

176 (Extended Data Fig. 5g) and repressed *PRR9* gene expression (Extended Data Fig. 5h-i). The

177 functional relevance of ELF4 movement was also verified in *elf4-1*(Sh)/*elf4-1*(Rt) grafts

178 showing the lack of rhythmic recovery in *elf4-1* roots when *elf4-1* was used as scion (Extended

179 Data Fig. 5j-k). Therefore, multiple series of evidence including the ELF4 injection data, the

180 grafting assays showing the recovery of the rhythms, the ELF4-GFP fluorescent signals across

181 the graft junctions, the detection of the ELF4 protein in roots of the grafted plants, the lack of

182 rhythmic recovery in roots of ELF4-x3GFP and in *elf4-1* scion grafts, support the notion that

183 ELF4 protein moves from shoots to regulate rhythms in roots. Other mobile proteins such as FT

184 (FLOWERING LOCUS T), and HY5 (LONG HYPOCOTYL 5) share some features with ELF4

185 protein in terms of low molecular weight and high isoelectric point (Fig. 2k).

186

187 **Blocking ELF4 movement by shoot excision alters circadian rhythms in roots**

188 We next attempted to unveil the function of the mobile ELF4 by blocking ELF4 movement

189 through shoot excision. Analyses of the rhythms showed that excised roots sustained robust

190 oscillations (Extended Data Fig. 6a-b) confirming that the root clock is able to run in the

191 absence of shoots. However, comparison of intact versus excised roots uncovered a shorter

192 period in excised roots (Extended Data Fig. 6c-d). As accumulation of ELF4 results in long

193 periods in shoots[22] and roots (Fig. 1e and Extended Data Fig. 1k), it is plausible that blocking

194 ELF4 movement by shoot excision leads to shorter periods in excised roots. If that is the case,

195 blocking ELF4 movement should also affect ELF4 target gene expression in excised roots.

196 Time course analyses by RT-QPCR revealed that the expression of *PRR9* and *PRR7* was up-

197 regulated in excised roots compared to intact roots (Extended Data Fig. 6e-f), which suggest

198 that in the absence of ELF4 movement from shoots, repression of these genes is alleviated in

199 roots. The use of ELF4-ox intact roots confirmed that *PRR9* and *PRR7* are targets of ELF4 as

200 their expression was clearly down-regulated in intact ELF4-ox roots compared to WT intact

201 roots (Extended Data Fig. 6g-h). Furthermore, ELF4-ox excised roots still showed repression of

202 target gene expression (Extended Data Fig. 6i-j) suggesting that excision *per se* is not

203 responsible for the up-regulation observed in WT excised roots.

204

205 To further uncover the function of ELF4 movement, we performed RNA-Seq analyses of WT

206 intact versus excised roots. Our results showed that as expected, a significant fraction of genes

207 was affected by excision (Suplementary Table 2). Comparative analyses of *elf4-1* intact roots

208 with WT excised roots allowed us to discern the effects due to excision from those due to the

209 lack of ELF4 movement (Extended Data Fig. 7). Indeed, we focused on the differentially

210 expressed genes (DEGs) present in both excised WT and intact *elf4-1* roots. As *elf4-1* mutant

211 roots are intact, the overlapping DEGs are not affected by excision *per se* but rather by the lack

212 of ELF4 movement from shoots, which is shared by *elf4-1* intact roots and WT excised roots.

213   Our comparative analyses of both datasets revealed that 67% of the DEGs in *elf4-1* intact roots
214   are also differentially expressed in WT excised roots (Supplementary Table 3) (Extended Data
215   Fig. 7). The proportion of overlapped DEGs (67%) is highly significant (P-value < 0.0001, chi-
216   square test for equality of proportions) as compared to the proportion of overlapping genes
217   (26%) using a random gene list. The overlap is noteworthy due to the different genotypes (*elf4-
218   1* mutant versus WT) and most importantly, the different conditions (intact versus excised). As
219   WT excised roots and *elf4-1* intact roots share the lack of ELF4 movement from shoots, the
220   overlapping DEGs provides a hint about genes that directly or indirectly require ELF4
221   movement for proper expression in roots. Consistently, the overlap of DEGs included nearly all
222   of the core oscillator genes (Suplementary Table 3 and Extended Data Fig. 6k). A significant
223   fraction of overlapped DEGs also circadianly oscillated with phase enrichments during the
224   subjective morning and subjective midday (Extended Data Fig. 6l). Therefore, ELF4 movement
225   appears to be important for a fully functional clock in roots.

226

227   **Mobile ELF4 does not regulate the photoperiodic-dependent phase in roots**
228   In aerial tissues, the circadian clock controls the photoperiodic regulation of growth and
229   development[50]. To determine whether ELF4 movement is important to deliver photoperiodic
230   information, we analyzed rhythms under short day (ShD) and long day (LgD) conditions. In
231   roots, *PRR9::LUC* waveforms displayed a subtle phase delay under LgD compared to ShD (Fig.
232   3a) following a similar trend to that observed in shoots (Fig. 3b). Time course analyses by
233   Western-blot of roots of ELF4 Minigene plants[20] confirmed the phase delay of ELF4 protein
234   accumulation under LgD compared to ShD (Fig. 3c-d). We reasoned that if ELF4 movement is
235   correlated with the photoperiodic-dependent phase delay, then excision of shoots might affect
236   the phase shift in roots. In agreement with the oscillations in promoter activity (Extended Data
237   Fig. 6c-d), the phase of ELF4 protein accumulation was advanced following excision under both
238   LgD and ShD (Extended Data Fig. 8a-d). Interestingly, under LgD conditions, excision
239   rendered a similar pattern of ELF4 accumulation than in intact roots under ShD (Fig. 3e-f).
240   Therefore, excision abolished the phase delay observed in intact root under LgD (compare Fig.
241   3c-d with Fig. 3e-f). The results suggest that the photoperiodic-dependent phase shift in roots is
242   hampered by blocking ELF4 movement. However, excised roots still showed the phase delay
243   under LgD compared to excised roots under ShD (Extended Data Fig. 8e-f). Furthermore,
244   analyses of rhythms under LgD conditions showed that plants mis-expressing ELF4 (ELF4-ox
245   and *elf4-1* mutant) displayed very similar rhythms to WT both in shoots and roots (Fig. 3g-h)
246   suggesting that ELF4 function is not essential to sustain rhythms under entraining conditions.
247   Together, the results suggest that blocking ELF4 movement by excision advances the phase of
248   the root clock but the mobile ELF4 does not directly regulate the photoperiodic-dependent
249   phase shift in roots.

250

ELF4 movement contributes to the temperature-dependent changes in circadian period of the root clock

As the EC also coordinates temperature responses, we examined whether a mobile ELF4 can convey temperature information from shoots to roots. To that end, we first examined the effect of different temperatures (28ºC, 18ºC and 12ºC) on circadian rhythms in roots. We found that *LHY::LUC* circadian period length was shorter at high than at low temperatures (Extended Data Fig. 9a-b). Shortening of period length at increasing temperature was also observed for other circadian reporter lines (Extended Data Fig. 9c-f) indicating that at this developmental stage and under our experimental conditions, the circadian clock in roots is not able to perfectly sustain circadian period length within a range of temperatures.

261

As ELF4 accumulation lengthens period length, we next examined the possible contribution of ELF4 to the long period phenotype at low temperatures. Changes in period length could be mediated by increased ELF4 activity and/or by the increased protein movement from shoots to roots. To examine these possibilities, we compared the effects of blocking ELF4 movement by excision at low and high temperatures. Essentially, if the long period in roots at 12ºC is independent of movement but results from the increased activity of ELF4, blocking movement from shoots by excision should not have a major effect on period length. However, if ELF4 movement contributes to the period regulation, abolishing ELF4 traffic should lead to an observable and differential effect on period length at different temperatures.

271

Our results showed that excision shortened the period length in WT roots and this effect was significant at 12ºC as compared to the minor effect at 28ºC (Extended Data Fig. 10a-d). Therefore, blocking ELF4 movement by excision shortens the long period of WT roots at 12ºC. Analyses of other circadian reporter lines and at 18ºC also showed that excision shortened period length compared to intact roots (Extended Data Fig. 10e-f). The results suggest a temperature-dependent control of ELF4 movement that regulates period length in roots. To further verify this notion, we examined rhythmic recovery in grafts of ELF4-ox scion into *elf4-1* rootstock at low and high temperatures. Our results showed an evident rhythmic recovery at 12ºC but not at 28ºC (Fig. 4a-b). Furthermore, grafts of E4MG scion into *elf4-1* rootstock also efficiently recovered rhythms at 12ºC but not at 28ºC (Fig. 4c-d). ELF4 is still able to delay the phase and lengthen the period at 28ºC (Fig. 4e and Extended Data Fig. 10g) suggesting that movement rather than changes in activity are responsible for the observed effects. ELF4 protein accumulation in roots of ELF4-ox scion into *elf4-1* rootstock was higher at 12ºC than at 28ºC (Figure 4f and Extended Data Fig. 10h-i) but ELF4 (E4MG) protein accumulation in shoots is

286 similar at different temperatures[31] (Extended Data Fig. 10j). Therefore, ELF4 movement rather
287 than protein accumulation or activity appears to be regulated by temperature, contributing to the
288 temperature-dependent control of circadian period in roots.

289

290 Altogether, we propose a model by which mobile ELF4 (mbE4) from shoots to roots defines a
291 pool of active ELF4 protein that is competent to repress target circadian gene expression in
292 roots. ELF4 trafficking is favored at low temperatures, which results in a slow-paced clock (Fig.
293 4g) while high temperatures decrease the movement, leading to a fast root clock (Fig. 4h). The
294 temperature-dependent movement of ELF4 allows a shoot-to-root dialogue that controls the
295 pace of the clock and provides a mechanism by which temperature cues from shoots set the
296 circadian period length in roots.

297

298 **Discussion**

299 The simultaneous examination of rhythms in shoots and roots of single individual plants shows
300 that the promoter activities and mRNA accumulation of clock genes in roots display a longer
301 period and delayed phase compared to shoots. The trend was observed for morning- and
302 evening-expressed key oscillator genes suggesting that the overall circadian system in roots is
303 not as precise as in other parts of the plant (e.g. the shoot apex)[47]. Despite the long period, the
304 rhythms persist in roots for several days under LL, which is reminiscent of a fully functional
305 clock. The lack of precision might provide circadian flexibility for rapid adjustments and
306 improved responses in roots. Previous studies have reported spatial waves of clock gene
307 expression with and within organs[40, 42, 45] that might be due to differences in period length and
308 variable local coupling.

309

310 The EC directly represses *PRR9* and *PRR7* expression[19, 23, 29, 51, 52] and indirectly promotes the
311 expression of the morning-expressed oscillator genes *CCA1* and *LHY*[51-54]. Our analyses with
312 *elf4-1* mutant and ELF4-ox plants demonstrate that ELF4 function in roots is also important for
313 proper repression of *PRR9* and *PRR7* and activation of *CCA1* and *LHY*. ELF4 regulatory
314 function in roots appears to be similar to that previously described for the EC using whole
315 plants. Over-expression of ELF4 lengthens the period of the root clock suggesting that ELF4
316 slows down the circadian period in roots as in shoots[22]. The fact that accumulation of ELF4
317 lengthens the period agrees with the results showing that blocking movement by shoot excision
318 shortens the period. RNA-Seq analyses revealed that not only the expression of oscillator genes
319 is affected in *elf4-1* roots but also a battery of genes involved in other pathways including
320 responses to stimuli. These pathways are also consistent with the EC function in responses to
321 environmental cues[55]. The mis-regulated genes in *elf4-1* roots might be direct targets of ELF4

322 and/or indirect outputs of the clock in roots. One of these outputs might be lateral root

323 emergence as the number of lateral roots is affected in *elf4-1* and ELF4-ox compared to WT.

324 Future studies are necessary to uncover the molecular and cellular mechanisms by which ELF4

325 regulates the number of lateral roots in Arabidopsis.

326

327 Micrografts of ELF4-ox scion into *elf4-1* or *elf4-2* rootstocks allow a remarkable recovery of

328 rhythms that is not observed when seedlings expressing ELF4 protein fused to 3 GFPs in

329 tandem is used as scion. These results suggest that ELF4 movement is indeed important for the

330 rhythmic recovery. Fluorescent signals accumulating in the vasculature of *elf4-1* mutant

331 rootstock grafted with ELF4-GFP scion and the detection of the ELF4 protein in roots of the

332 micrografted plants also suggest that ELF4 moves from shoots to roots. This conclusion is

333 complemented with the grafting assays of *elf4-1*(Sh)/*elf4-1*(Rt) showing the lack of rhythmic

334 recovery in roots, and with the assays of ELF4 protein injection in shoots and the subsequent

335 rhythmic recovery in roots. Micrografts of E4MG and WT plants are also able to recover the

336 rhythms of the *elf4-1* mutant roots, which indicate that the effects are not due to the over-

337 accumulation of ELF4-ox and suggest that the amount of mobile ELF4 that is required to

338 regulate the rhythms is probably not very high. Our experiments adding water to the scion or

339 using WT scion without LUC reporter exclude the possibility that rhythms in grafted roots are

340 due to leakage for the adjacent well containing the shoot. The fact that ELF4 protein shows

341 similar properties in terms of length, molecular weight and isoelectric point to other mobile

342 proteins[56-59] also support the notion of ELF4 movement. We postulate that following movement,

343 the complex regulatory feedback loops at the core of the oscillator will be reset to control the

344 pace of the clock. Further experiments at different developmental stages and various growing

345 conditions (e.g. light and temperature) will be required to confirm whether the long distance

346 movement of ELF4 contributes or not to the spatial waves of clock gene expression observed in

347 roots[42].

348

349 Excision blocks ELF4 movement from shoots and consequently, we observe that oscillator gene

350 expression and other output genes are affected in WT excised roots. Previous studies have also

351 used excision to define properties of the circadian function in roots[42]. Although many genes are

352 affected by excision, it is noteworthy that 67% of the genes mis-regulated in *elf4-1* intact roots

353 are also mis-expressed in WT excised roots. Both conditions share the lack of ELF4 movement,

354 which suggest that the overlapped DEGs are due to the lack of a mobile ELF4 (note that the

355 RNA-Seq studies with *elf4-1* mutant were performed with intact roots). The phase shifts

356 observed following excision prompted us to examine whether ELF4 movement contributed to

357 the photoperiodic-dependent phase shift. However, excised roots still sustained the phase delay

358 under LgD suggesting that other factors are responsible for this regulation. Light piping down

359 the root[49] might be also important for synchronization. Regardless the mechanism, it is able to

360 overcome the mis-expression of ELF4 in shoots and roots as ELF4-ox and *elf4-1* mutant plants

361 displayed similar rhythms to WT. Clear alteration of circadian expression under LL but not

362 under entraining conditions has been reported for other clock mutants and over-expressing

363 plants[60].

364

365 The EC activity is down-regulated at high temperatures in whole seedlings[29, 31]. Shoot excision

366 shortened the period, suggesting that ELF4 movement is important in the control of circadian

367 period length. Period shortening is more significant at low than at high temperatures confirming

368 that ELF4 movement might be favored at low temperatures. The temperature-dependent control

369 of ELF4 movement is also supported by the increased accumulation ELF4 protein in grafted

370 roots at 12ºC compared to 28ºC. As ELF4 accumulation results in long period, the increased

371 movement leads to a clock that runs slower at low than at high temperatures. It would be

372 interesting to elucidate whether period sensitivity to temperature might provide an advantage for

373 optimal root responsiveness to temperature variations.

374

375 **Methods**

376 **Plant material, growth conditions, constructs and physiological assays**

377 *Arabidopsis thaliana* seedlings were stratified at 4°C in the dark for 2-3 days on Murashige and

378 Skoog (MS) agar medium with 3% of sucrose (MS3). Plates were transferred to chambers with

379 light- and temperature-controlled conditions with 25-50 µmol·quanta·m^{-2}·s^{-1} of cool white

380 fluorescent light. Seedlings were synchronized under Light:Dark cycles, LD (12h light: 12h

381 dark) at 22°C. For experiments with different temperatures, seedlings were analyzed under

382 constant light conditions at 12ºC, 18ºC, 22ºC or 28ºC following synchronization under LD (12h

383 light: 12h dark) at 22°C. For experiments with different photoperiods, seedlings were grown

384 under short days (ShD, 8h light: 16h dark) or long days (LgD, 16h light: 8h dark). Reporter

385 lines *CCA1::LUC*[61], *LHY::LUC*[19], *PRR9::LUC*[62], *TOC1::LUC*[6] and *elf4-1*[17], *elf4-2*[27], ELF4

386 Minigene[20] and ELF4-GFP-ox[19, 20] plants were described elsewhere. The ELF4 construct fused

387 to three Green Fluorescent Proteins (GFPs) in tandem was generated by PCR-mediated

388 amplification of the *ELF4* coding sequence and subsequent subcloning into the PGWB514

389 gateway vector[63, 64]. The resulting plasmid was digested with PacI and SacI restriction enzymes

390 and ligated with the 3 GFPs insert from the pBS-x3GFP vector (Addgene). The construct was

391 transformed into *elf4-1* mutant plants. Plants were transformed using *Agrobacterium*

392 *tumefaciens* (GV2260)-mediated DNA transfer[65]. For in vitro protein injection assays, the ELF4

393 coding sequence was subcloned into the pET MBP_1a vector (Novagen) after removing the

394 GFP by Nco I and Xho I restriction enzyme digestion.

395

396   For lateral root analyses, WT, *elf4-1* and ELF4-ox seeds were surface-sterilized and plated onto

397   MS medium supplemented with 0.25% w/v sucrose and 1.5% agar. The top quarter of the agar

398   was removed and seeds pipetted evenly along this line. Plants were then grown vertically for 12

399   days before lateral roots were measured. Lateral roots were manually counted using a Nikon

400   SMZ800 dissecting microscope. Statistical analysis was completed using R (version 3.6), within

401   the R studio software package (version 1.1.4). For hypocotyl elongation measurements, WT,

402   *elf4-1*, ELF4-GFP-ox and ELF4-3xGFP-ox seeds transformed into the *elf4-1* mutant

403   background were stratified on MS3 medium in the dark for 4 days at 4°C, exposed to white light

404   (40 μmol·quanta·m^{-2}·s^{-1}) for 6 h and maintained in the dark (22ºC) for 18 h before transferring

405   to chambers under Short-Day conditions (8h light:16h dark). Hypocotyl length was measured

406   using the ImageJ software (version 1.48v) (https://imagej.nih.gov/ij/) at 7 days after

407   stratification. Each experiment was repeated at least twice using 20-50 seedlings per genotype.

408   Statistical analyses were performed using the GraphPad Prism software (version 5.01;

409   GraphPad Software, Inc) using two-tailed t-tests with 95% of confidence.

410

411   **In vivo luminescence assays**

412   In vivo luminescence assays were performed as previously described[47]. Briefly, 7-15 day-old

413   seedlings synchronized under LD cycles at 22°C were transferred to 96-well plates and released

414   into the different conditions as specific for each experiment. Analyses were performed with a

415   LB960 luminometer (Berthold Technologies) using the Microwin software (Version 4.41;

416   Mikrotek Laborsysteme). The period, phase and amplitude were estimated using the Fast

417   Fourier Transform–Non☐Linear Least Squares (FFT☐NLLS) suite 63[66] using the Biological

418   Rhythms Analysis Software System (version 3.0; BRASS, http://www.amillar.org). For the

419   simultaneous analysis of rhythms of shoots and roots from the same plant, the connection

420   between the two adjacent wells of the 96☐well plates was serrated. Seedlings were then

421   horizontally positioned so the shoot was placed in one well and the roots in the contiguous well.

422   For excision analyses, roots were excised from shoots and placed into the 96☐well plates for

423   luminescence analyses. Data from samples that appeared damaged or contaminated were

424   excluded from the analysis. For analyses of grafted samples, water instead of luciferin was

425   applied to the wells containing shoots to avoid possible leaking signals from shoots to roots as

426   specified. At least two biological replicates were performed per experiment, with measurements

427   taken from distinct samples grown and processed at different times. Each biological replicate

428   included 6 to 12 independent seedlings per condition and/or genotype. Statistical analyses were

429   performed using the GraphPad Prism software (version 5.01; GraphPad Software, Inc) using

430   two-tailed t-tests with 95% of confidence.

431

432

Protein purification and injection analyses

433

E. coli cells (BL21, Dh5α) were transformed and grown in LB medium (Tryptone 10 g/L, yeast

434

extract 5 g/L, NaCl 10 g/L pH 7.5) until OD600 values of 0.8-1.0. Isopropyl β-D-1-

435

thiogalactopyranoside (IPTG)-mediated induction of MBP-ELF4 and MBP-GFP was performed

436

at 28ºC for 6 h. Bacteria resupended in lysis buffer (50mM Tris-HCl, pH7-8, 5% glycerol,

437

50mM NaCl) were lysed by sonication for 2-3 minutes (30s on, 30s off, high intensity) using a

438

sonicator (Bioruptor, Diagnode). Recombinant proteins were purified using gravity flow

439

columns with amylose resin (New England Biolabs). MBP cleavage was performed by

440

incubation in cleavage buffer (50 mM Trizma-HCl, pH 8.0, 0.5 mM EDTA, and 1 mM DTT)

441

for 2 hours at 30ºC with native Tobacco Etch Virus (TEV) protease (Sigma-Aldrich). The

442

purified recombinant proteins were concentrated using Amicon centrifugal filters following the

443

manufacturer recommendations (Millipore). Protein yield was estimated by measuring

444

absorbance at 595 nm using a spectrophotometer (UV-2600, SHIMADZU). Proteins were also

445

examined by Coomassie-Brilliant Blue staining of polyacrylamide gels to confirm protein size

446

and integrity. Purified ELF4 was injected into leaves of 10-day old *elf4-1* mutant seedlings

447

harboring the *LHY::LUC* reporter line. Similar concentration of GFP protein was also injected

448

as a negative control. Rhythms were subsequently examined in a LB960 luminometer (Berthold

449

Technologies) as described above.

450

451

Time course analyses of gene expression by RT-qPCR

452

Seedlings were synchronized under LD cycles in MS3 medium plates for 12-14 days and

453

subsequently transferred to LL. Shoots and roots from intact plants were taken every 4 hour

454

over the circadian cycle. For excised roots, shoots and roots were carefully separated with a

455

sterile razor blade and the excised roots were deposited on MS3 agar medium plates for 2 or 3

456

days as specified. RNA was purified using a Maxwell RSC Plant RNA kit following the

457

manufacturer's recommendations (Promega). Single-stranded cDNA was synthesized using

458

iScript Reverse Transcription Supermix for RT-qPCR (Bio-Rad). qPCR analyses were

459

performed with cDNAs diluted 50☐fold with nuclease☐free water using Brilliant III Ultra-Fast

460

SYBR Green qPCR Master Mix (Agilent) with a 96-well CFX96 Touch Real-Time PCR

461

detection system (Bio-RAD CFX96 Manager version 3.1, Bio-Rad). Each sample was run in

462

technical triplicates. The expression of *PP2AA3 (PROTEIN PHOSPHATASE 2A SUBUNIT A3,*

463

AT1G13320) or *MON1* (*MONENSIN SENSITIVITY1*, AT2G28390)[67] was used as a control.

464

Crossing point (Cp) calculation was used for quantification using the Absolute Quantification

465

analysis by the 2nd Derivative Maximun method. At least two biological replicates were

466

467 performed, with measurements taken from distinct samples grown and processed at different
468 times.

469

470 **RNA☐Seq analyses**

471 Roots from 14-day old intact WT, *elf4-1* mutant and excised WT plants synchronized under LD
472 cycles in MS3 medium plates were transferred to LL conditions for 3 days. Roots were excised
473 just before transferring to LL. Samples were collected at the fourth day under LL at circadian
474 time 75 (CT75). Total RNA was isolated using a Maxwell RSC Plant RNA kit. RNA
475 sequencing was performed by IGATech (Italy). About 1-2 μg of high quality RNA (R.I.N. >7)
476 was used for library preparation with a TruSeq Stranded mRNA Sample Prep kit' (Illumina, San
477 Diego, CA). Poly-A mRNA was fragmented for 3 minutes at 94°C. Purification was performed
478 with 0.8x Agencourt AMPure XP beads. Both RNA samples and final libraries were quantified
479 using the Qubit 2.0 Fluorometer (Invitrogen, Carlsbad, CA). Quality was tested using the
480 Agilent 2100 Bioanalyzer RNA Nano assay (Agilent technologies, Santa Clara, CA). Libraries
481 were then processed with Illumina cBot for cluster generation on the flowcell, following the
482 manufacturer's instructions and sequenced on paired-end mode at the multiplexing level
483 requested on HiSeq2500 (Illumina, San Diego, CA). The CASAVA (1.8.2 version) of the
484 Illumina pipeline was used to process raw data for both format conversion and de-multiplexing.

485

486 Sequence analysis was performed using the A.I.R. software (version 1.0)
487 (https://transcriptomics.sequentiabiotech.com/) developed by Sequentia Biotech. Briefly, raw
488 sequence files were first subjected to quality control analysis by using FastQC (v0.10.1) before
489 trimming and removal of adapters with BBDuk (https://jgi.doe.gov/data-and-tools/bbtools/).
490 Reads were then mapped against the *Arabidopsis thaliana* genome (TAIR10 Genome Release,
491 ftp://ftp.arabidopsis.org/) with STAR (version 2.6)[68]. FeatureCounts (version 1.6.1)[69] was then
492 used to obtain raw expression counts for each annotated gene. The differential expression
493 analysis was conducted with edgeR (version 3.18.1)[70], using the TMM normalization method.
494 FPKM were obtained with edgeR.

495

496 The Integrative Genomics Viewer (IGV, version 2.4.13)
497 (https://software.broadinstitute.org/software/igv/) was used to visualize the data[74, 75]. The
498 circadian phases were analyzed using the publicly available Gene Phase Analysis Tool
499 "PHASER" of the DIURNAL database (http://diurnal.mocklerlab.org/)[76, 77]. Phase over☐
500 representation is calculated as the number of genes with a given phase divided by the total
501 number of genes over the number of genes called rhythmic and divided by the total number of
502 genes in the dataset. Functional categories of the DEG were obtained using the web tool
503 "BIOMAPS"(VirtualPlant, version 1.3)[78], which renders over☐represented and significant

504 functional terms (Gene Ontology or MIPS) as compared to the frequency of the term in the
505 whole genome.

506

507 **Western-blot assays**

508 Approximately 50-100 mgs of roots from plants grown under the specified photoperiodic
509 condition were sampled every four hours over a 24-hour cycle. Samples were rapidly frozen
510 with liquid nitrogen and grounded with stainless steel beads (Millipore) in a tissue lyser
511 (QIAGEN, TissueLyser II). Tissue was subsequently resuspended in Protein Extraction Buffer
512 (PEB) containing 50 mM Tris-HCl pH 7.5, 150 mM NaCl, 0.5% NP40, 1 mM EDTA, and
513 protease inhibitors cocktail (1:100) and PMSF (1:1000). Protein extracts were centrifuged at
514 4 °C, measured for protein concentration using Bradford reagent (Bio-Rad) and normalized to 2
515 mg/ml in 4 x SDS loading buffer (250 mM Tris-HCl, pH 6.8, 8% SDS, 0.08% bromophenol
516 blue, 40% glycerol). Samples were run on a 12% gel and analyzed by immunoblotting, fixed 30
517 min with 0.4% Glutaraldehyde solution (Sigma-Aldrich) and detected with an anti-HA antibody
518 (Roche) (1:2000 dilution) and a goat anti-rat horse peroxidase conjugated secondary antibody
519 (Sigma-Aldrich) (1:4000 dilution). For analyses of the grafted plants, roots from plants
520 synchronized under LD cycles were subsequently transferred to LL for 3 days at 12ºC, 22ºC or
521 28ºC. Samples were collected at CT81, rapidly frozen with liquid nitrogen and grounded with
522 stainless steel beads (Millipore) in a tissue lyser (QIAGEN, TissueLyser II). Powder extracts
523 were subsequently resuspended in Protein Extraction Buffer (PEB) containing 50 mM Tris-HCl
524 pH 7.5, 150 mM NaCl, 0.5% NP40, 1 mM EDTA, and protease inhibitors cocktail (1:100),
525 PMSF (1:1000), and MG132 (100uM). Protein extracts were centrifuged at 4 °C, measured for
526 protein concentration using Bradford reagent (Bio-Rad) and normalized to 2 μg/ μl in 4 x SDS
527 loading buffer (250 mM Tris-HCl, pH 6.8, 8% SDS, 0.08% bromophenol blue, 40% glycerol
528 and 5 mM β-mercaptoethanol). For detection of ELF4 protein fused to GFP, samples were run
529 on a 10% gel and was detected using an anti-GFP antibody (ab290, Abcam) (1:5000) and Goat
530 anti-Rabbit IgG (H+L) Secondary Antibody, HRP (31460, Lot: OG188649, Thermo Fisher
531 Scientific) (1:5000 dilution).. For detection of ELF4 protein fused to HA (ELF4 Minigene) in
532 shoots, samples were resuspended in Protein Extraction Buffer (PEB) containing 50mM
533 TrisHCl pH7.5, 150mM NaCl, 0.5% NP40, 1mM EDTA, protease inhibitors and proteasome
534 inhibitor (MG132, 100uM). Protein extracts in 4× SDS loading buffer (250 mM Tris-HCl, pH
535 6.8, 8% SDS, 0.08% bromophenol blue, 40% glycerol, 5 mM β-mercaptoethanol) were run on a
536 12% gel and analyzed by immunoblotting, fixed 30 min with 0.4% Glutaraldehyde solution
537 (Sigma-Aldrich) and detected with an Anti-HA antibody High Affinity from rat IgG1
538 (11867423001, Sigma-Aldrich) (1:2000) and a goat anti-rat horse peroxidase conjugated
539 secondary antibody (A9037, Sigma-Aldrich) (1:4000). The Image Lab software (version 5.2.1;
540 Bio-Rad) was used to image the Western-blots. Membranes were stained with a Ponceau S

541 solution following the manufacturer recommendations (Sigma). Proteins were also run on a

542 10% SDS-PAGE gel and stained with Coomassie-Brilliant Blue. At least two biological

543 replicates were performed per experiment and/or condition, with measurements taken from

544 distinct samples grown and processed at different times.

545

546 **Micrografting assays**

547 Micrografting was performed essentially as previously described[47]. Data from unsuccessful

548 grafted seedlings that failed to properly join together or grafts that were insufficiently clear to be

549 successful were discarded. Approximately 100-150 grafting events were performed for every

550 combination of grafts. The percentage of successfully micrografted plants was about 30-50 %

551 (possibly higher but only the clearly successful grafted plants were taken into account). From

552 the successfully grafted plants, 30-60 % showed different degrees of recovered rhythms. For in

553 vivo luminescence assays, shoots and roots of grafted plants were simultaneously examined

554 using the protocol described above. Water instead of luciferin was added to the wells containing

555 shoots to exclude the possibility that recovery of rhythms in roots were due to leaking signals

556 from shoots. As specified, some grafted shoots contained no reporter fused to luciferase.

557

558 **Reconstruction of driving forces by recurrence plots**

559 Common driving forces were estimated following a several-step procedure. Suppose that we

560 have the number K of simultaneous time series measurements $\{s_i(t)|i = 1,2,...,K, t =$

561 $1,2,...,T\}$. First, we took time differences $\tilde{s}_i(t) = s_i(t+1) - s_i(t)$ ($i = 1,2,...,K, t =$

562 $1,2,...,T-1$) of consecutive measurements and remove trends. Second, we used delay

563 coordinates[79, 80] $\vec{s}_i(t) = [\tilde{s}_i(t), \tilde{s}_i(t+1), \tilde{s}_i(t+2), \tilde{s}_i(t+3), \tilde{s}_i(t+4)]$ of 5 dimensional space

564 ($i = 1,2,...,K, t = 1,2,...,T-4$) to obtain a recurrence plot[81]. A recurrence plot is a two-

565 dimensional figure proposed originally for visualizing time series data. Both axes are the same

566 time axis. If the Euclidean distance $\|\vec{s}_i(t_1) - \vec{s}_i(t_2)\| < \varepsilon_i$, where ε_i is a threshold and $t_1, t_2 \in$

567 $\{1,2,...,T-4\}$, then we plot a point at (t_1, t_2). We denote this as $R_i(t_1, t_2) = 1$. Otherwise, we

568 do not plot a point at (t_1, t_2). We denote this state as $R_i(t_1, t_2) = 0$. We controlled the value of

569 the threshold ε_i for each component $i \in \{1,2,...,K\}$ so that 5% points, except for the central

570 diagonal line, have points plotted. Third, we took the union for the recurrence plots to infer the

571 recurrence plot of the common driving force[82]. Namely we declare $R(t_1, t_2) = 1$ if we have

572 $R_i(t_1, t_2) = 1$ for at least one of $i \in \{1,2,...,K\}$. Otherwise, we have $R(t_1, t_2) = 0$. In each of

573 the original recurrence plots, points are plotted where the driving force and the driven system

574 are both similar. By taking their union, we can extract pairs of times where only the driving

575 force is similar. Fourth, we applied the assumption of continuity and supplied the points at

576 (t,t+1) and (t+1,t) for each i[83]. Namely, we forcefully declare $R(t, t+1) = R(t+1, t) = 1$ for

577   $t = 1, 2, \ldots, T - 5$. Fifth, we applied the method described[82] to convert the recurrence plot of the

578   common driving force into time series. Here we describe the detail for this step: (i) we construct

579   a network where each node correspond to a time point and we connect two nodes t_1 and t_2 if

580   $R(t_1, t_2) = 1$; (ii) we assign a distance for each edge as $1 - \frac{\#\{k=1,2,\ldots,T-4 | R(k,t_1)=1 \text{ and } R(k,t_2)=1\}}{\#\{k=1,2,\ldots,T-4 | R(k,t_1)=1 \text{ or } R(k,t_2)=1\}}$,

581   (iii) we obtain the shortest distance for each pair of nodes on this graph (this process

582   approximates the geodesic distance between two time points); (iv) we apply the multi-

583   dimensional scaling to convert the distance matrix to a time series. Namely this fifth step works

584   as the inverse transform of a recurrence plot and we can reproduce a rough shape for the

585   original time series. This fifth step has two mathematical proofs[84, 85]. Lastly, we extracted the

586   component corresponding to the largest eigenvalue. The periodicity of the reconstructed

587   common driving force X(t) was evaluated using the autocorrelation function and 10000 random

588   shuffle surrogates[86], for each of which the order of time points is randomly exchanged. Here, the

589   null hypothesis was that there was no serial dependence. The autocorrelation with time

590   difference k is the correlation coefficient between X(t) and X(t+k). Thus, it is close to 1 if X(t)

591   and X(t+k) are similar while it is close to 0 if they are not related to each other. If there is a 24h

592   periodicity in the driving force, the autocorrelation with 24h time difference should be a value

593   close to 1.

594   **Confocal imaging**

595   For *in vivo* confocal imaging, the roots of WT and ELF4-ox (fused to GFP) grafted shoots into

596   *elf4-1* mutants were placed on microscope slides (Sigma). Fluorescent signals were imaged with

597   an argon laser (transmissivity: 40%; excitation: 515 nm; emission range: 530□630 nm) in a

598   FV□1000 confocal microscope (Olympus, Tokyo, Japan) using a FV-10-ASW4.2 Viewer

599   Manager software (Olympus) with a 40x/1.3 oil immersion objective. The image sizes were

600   about 640 x 640 (0.497 μm/pixel) and sampling speed of 4 μs/pixel. The results are

601   representative of at least three biological replicates for grafting and about three-four images per

602   grafts.

603

604   **List of primers.** List of primers used for expression analyses, cloning and generation of 3x GFP

605   construct.

Name	Sequence	Experiment
REF1(PP2A_A3)_EXP_F	AAGCGGTTGTGGAGAACATGATACG	Expression analysis
REF1(PP2A_A3)_EXP_R	TGGAGAGCTTGATTTGCGAAATACCG	Expression analysis
MON1_EXP_F	AACTCTATGCAGCATTTGATCCACT	Expression analysis
MON1_EXP_R	TGATTGCATATCTTTATCGCCATC	Expression analysis
PRR7_EXP_F	AAGTAGTGATGGGAGTGGCG	Expression analysis
PRR7_EXP_R	GAGATACCGCTCGTGGACTG	Expression analysis
PRR9_EXP_F	ACCAATGAGGGGATTGCTGG	Expression analysis

PRR9_EXP_R	TGCAGCTTCTCTCTGGCTTC	Expression analysis
ELF4_EXP_F	GACAATCACCAATCGAGAAT	Expression analysis
ELF4_EXP_R	ATGTTTCCGTTGAGTTCTTG	Expression analysis
CCA1_EXP_F	TCGAAAGACGGGAAGTGGAACG	Expression analysis
CCA1_EXP_R	GTCGATCTTCATTGGCCATCTCAG	Expression analysis
LHY_EXP_F	AAGTCTCCGAAGAGGGTCGT	Expression analysis
LHY_EXP_R	GGCGAAAAGCTTTGAGGCAA	Expression analysis
ELF4_CLN_F	CACCATGAAGAGGAACGGCGA	Cloning
ELF4_CLN_R	AGCTCTAGTTCCGGCAGCACCA	Cloning
MBP-ELF4_CLN_F	CATGCCATGGGCATGAAGAGGAACGGCGAG	Cloning
MBP-ELF4_CLN_R	CCGCTCGAGTTAAGCTCTAGTTCCGGCAGCAC	Cloning
PacI-pBS3xGFP-F	GGTTAATTAACGCTGGAGGATCCATGTCTA	Generation of pGWB-c3xGFP
SacI-pBS3xGFP-R	TCGAGCTCTCTAGAACTAGTGGATCTTTA	Generation of pGWB-c3xGFP

606

607

Reporting Summary. Further information on research design is available in the Nature Research Reporting Summary linked to this article.

610

Data availability

Data and materials generated in this study are available without restriction and should be requested to Paloma Mas: paloma.mas@cragenomica.es. NGS data are deposited in NCBI with accession code PRJNA610472 (BioSample accessions SAMN14299292, SAMN14299293, SAMN14299294). Source data are provided for all figures.

616

References

1. Zhang, E.E. & Kay, S.A. Clocks not winding down: unravelling circadian networks. *Nat. Rev. Mol. Cell. Biol.* **11**, 764-776 (2010).
2. Greenham, K. & McClung, C.R. Integrating circadian dynamics with physiological processes in plants. *Nat. Rev. Genet.* **16**, 598-610 (2015).
3. Nagel, Dawn H. & Kay, Steve A. Complexity in the wiring and regulation of plant circadian networks. *Curr. Biol.* **22**, R648-R657 (2012).
4. Oakenfull, R.J. & Davis, S.J. Shining a light on the Arabidopsis circadian clock. *Plant Cell Environ* **40**, 2571-2585 (2017).
5. Hogenesch, J.B. & Ueda, H.R. Understanding systems-level properties: timely stories from the study of clocks. *Nature Reviews Genetics* **12**, 407 (2011).
6. Portolés, S. & Más, P. The functional interplay between protein kinase CK2 and CCA1 transcriptional activity is essential for clock temperature compensation in Arabidopsis. *PLoS Genetics* **6**, e1001201 (2010).
7. Hansen, L.L., van den Burg, H.A. & van Ooijen, G. Sumoylation Contributes to Timekeeping and Temperature Compensation of the Plant Circadian Clock. *J Biol Rhythms* **32**, 560-569 (2017).
8. Marshall, C.M., Tartaglio, V., Duarte, M. & Harmon, F.G. The Arabidopsis *sickle* Mutant Exhibits Altered Circadian Clock Responses to Cool Temperatures and Temperature-Dependent Alternative Splicing. **28**, 2560-2575 (2016).

637　9.　　Salomé, P., Weigel, D. & McClung, C. The role of the Arabidopsis morning loop
638　　　　components CCA1, LHY, PRR7, and PRR9 in temperature compensation. *Plant Cell*
639　　　　**22**, 3650-3661 (2010).
640　10.　　Edwards, K.D., Lynn, J.R., Gyula, P., Nagy, F. & Millar, A.J. Natural allelic variation
641　　　　in the temperature-compensation mechanisms of the *Arabidopsis thaliana* circadian
642　　　　clock. *Genetics* **170**, 387-400 (2005).
643　11.　　Edwards, K.D. *et al.* FLOWERING LOCUS C mediates natural variation in the high-
644　　　　temperature response of the Arabidopsis circadian clock. *Plant Cell* **18**, 639 - 650
645　　　　(2006).
646　12.　　Ito, S. *et al.* FLOWERING BHLH transcriptional activators control expression of the
647　　　　photoperiodic flowering regulator *CONSTANS* in Arabidopsis. **109**, 3582-3587 (2012).
648　13.　　Gould, P.D. *et al.* Network balance via CRY signalling controls the Arabidopsis
649　　　　circadian clock over ambient temperatures. **9**, 650 (2013).
650　14.　　Nagel, D.H., Pruneda-Paz, J.L. & Kay, S.A. FBH1 affects warm temperature responses
651　　　　in the Arabidopsis circadian clock. **111**, 14595-14600 (2014).
652　15.　　Jones, M.A., Morohashi, K., Grotewold, E. & Harmer, S.L. Arabidopsis JMJD5/JMJ30
653　　　　Acts Independently of LUX ARRHYTHMO Within the Plant Circadian Clock to
654　　　　Enable Temperature Compensation. **10** (2019).
655　16.　　Gould, P.D. *et al.* The molecular basis of temperature compensation in the Arabidopsis
656　　　　circadian clock. *Plant Cell* **18**, 1177-1187 (2006).
657　17.　　Doyle, M.R. *et al.* The ELF4 gene controls circadian rhythms and flowering time in
658　　　　*Arabidopsis thaliana*. *Nature* **419**, 74-77 (2002).
659　18.　　Kolmos, E. *et al.* Integrating ELF4 into the circadian system through combined
660　　　　structural and functional studies. *HFSP journal* **3**, 350-366 (2009).
661　19.　　Herrero, E. *et al.* EARLY FLOWERING4 recruitment of EARLY FLOWERING3 in
662　　　　the nucleus sustains the Arabidopsis circadian clock. *Plant Cell* **24**, 428-443 (2012).
663　20.　　Nusinow, D.A. *et al.* The ELF4-ELF3-LUX complex links the circadian clock to
664　　　　diurnal control of hypocotyl growth. *Nature* **475**, 398-402 (2011).
665　21.　　Khanna, R., Kikis, E.A. & Quail, P.H. EARLY FLOWERING 4 functions in
666　　　　phytochrome B-regulated seedling de-etiolation. *Plant Physiol.* **133**, 1530-1538 (2003).
667　22.　　McWatters, H.G. *et al.* ELF4 is required for oscillatory properties of the circadian
668　　　　clock. *Plant Physiol.* **144**, 391-401 (2007).
669　23.　　Helfer, A. *et al.* LUX ARRHYTHMO encodes a nighttime repressor of circadian gene
670　　　　expression in the Arabidopsis core clock. *Curr. Biol.* **21**, 126-133 (2011).
671　24.　　Onai, K. & Ishiura, M. PHYTOCLOCK 1 encoding a novel GARP protein essential for
672　　　　the Arabidopsis circadian clock. *Genes Cells* **10**, 963-972 (2005).
673　25.　　Hazen, S.P. *et al.* LUX ARRHYTHMO encodes a Myb domain protein essential for
674　　　　circadian rhythms. *Proc. Natl. Acad. Sci. USA* **102**, 10387-10392 (2005).
675　26.　　Hicks, K.A. *et al.* Conditional circadian dysfunction of the *Arabidopsis early-flowering
676　　　　3* mutant. *Science* **274**, 790-792 (1996).
677　27.　　Huang, H. *et al.* Identification of Evening Complex associated proteins in Arabidopsis
678　　　　by affinity purification and mass spectrometry. *M. Cell. Proteomics* **15**, 201-217 (2016).
679　28.　　Li, G. *et al.* Coordinated transcriptional regulation underlying the circadian clock in
680　　　　Arabidopsis. *Nat. Cell Biol.* **13**, 616-622 (2011).
681　29.　　Mizuno, T. *et al.* Ambient temperature signal feeds into the circadian clock
682　　　　transcriptional circuitry through the EC night-time repressor in Arabidopsis thaliana.
683　　　　*Plant Cell Physiol.* **55**, 958-976 (2014).
684　30.　　Siddiqui, H., Khan, S., Rhodes, B.M. & Devlin, P.F. FHY3 and FAR1 act downstream
685　　　　of light stable phytochromes. *Front Plant Sci.* **7**, 175 (2016).
686　31.　　Ezer, D. *et al.* The evening complex coordinates environmental and endogenous signals
687　　　　in Arabidopsis. *Nat. Plants* **3**, 17087 (2017).
688　32.　　Kim, Y. *et al.* ELF4 Regulates GIGANTEA Chromatin Access through Subnuclear
689　　　　Sequestration. *Cell Reports* **3**, 671-677 (2013).

690   33.   Nieto, C., López-Salmerón, V., Davière, J.-M. & Prat, S. ELF3-PIF4 Interaction
691   Regulates Plant Growth Independently of the Evening Complex. *Current Biology* **25**,
692   187-193 (2015).
693   34.   Sai, J. & Johnson, C.H. Different circadian oscillators control Ca(2+) fluxes and lhcb
694   gene expression. *Proc. Natl. Acad. Sci. USA* **96**, 11659-11663 (1999).
695   35.   Thain, S.C., Murtas, G., Lynn, J.R., McGrath, R.B. & Millar, A.J. The circadian clock
696   that controls gene expression in Arabidopsis is tissue specific. *Plant Physiol.* **130**, 102-
697   110 (2002).
698   36.   Michael, T.P., Salome, P.A. & McClung, C.R. Two Arabidopsis circadian oscillators
699   can be distinguished by differential temperature sensitivity. *Proc. Natl. Acad. Sci. USA*
700   **100**, 6878-6883 (2003).
701   37.   Bordage, S., Sullivan, S., Laird, J., Millar, A.J. & Nimmo, H.G. Organ specificity in the
702   plant circadian system is explained by different light inputs to the shoot and root clocks.
703   *New Phytol.* **212**, 136-149 (2016).
704   38.   Muranaka, T. & Oyama, T. Heterogeneity of cellular circadian clocks in intact plants
705   and its correction under light-dark cycles. *Sci. Adv.* **2**, e1600500 (2016).
706   39.   Thain, S.C., Hall, A. & Millar, A.J. Functional independence of circadian clocks that
707   regulate plant gene expression. *Curr. Biol.* **10**, 951-956 (2000).
708   40.   Fukuda, H., Nakamichi, N., Hisatsune, M., Murase, H. & Mizuno, T. Synchronization
709   of plant circadian oscillators with a phase delay effect of the vein network. *Phys. Rev.*
710   *Lett.* **99**, 098102 (2007).
711   41.   Wenden, B., Toner, D.L.K., Hodge, S.K., Grima, R. & Millar, A.J. Spontaneous
712   spatiotemporal waves of gene expression from biological clocks in the leaf. *Proc. Natl.*
713   *Acad. Sci.* **109**, 6757-6762 (2012).
714   42.   Greenwood, M., Domijan, M., Gould, P.D., Hall, A.J.W. & Locke, J.C.W. Coordinated
715   circadian timing through the integration of local inputs in Arabidopsis thaliana. *PLOS*
716   *Biology* **17**, e3000407 (2019).
717   43.   Endo, M., Shimizu, H., Nohales, M.A., Araki, T. & Kay, S.A. Tissue-specific clocks in
718   Arabidopsis show asymmetric coupling. *Nature* **515**, 419-422 (2014).
719   44.   Yakir, E. *et al.* Cell autonomous and cell-type specific circadian rhythms in
720   Arabidopsis. *Plant J.* **68** 520-531 (2011).
721   45.   Gould, P.D. *et al.* Coordination of robust single cell rhythms in the Arabidopsis
722   circadian clock via spatial waves of gene expression. *Elife* **7**, e31700 (2018).
723   46.   Fukuda, H., Ukai, K. & Oyama, T. Self-arrangement of cellular circadian rhythms
724   through phase-resetting in plant roots. *Phys. Rev. E.* **86**, 041917 (2012).
725   47.   Takahashi, N., Hirata, Y., Aihara, K. & Mas, P. A hierarchical multi-oscillator network
726   orchestrates the Arabidopsis circadian system. *Cell* **163**, 148-159 (2015).
727   48.   James, A.B. *et al.* The circadian clock in Arabidopsis roots is a simplified slave version
728   of the clock in shoots. *Science* **322**, 1832-1835 (2008).
729   49.   Nimmo, H.G. Entrainment of Arabidopsis roots to the light:dark cycle by light piping.
730   *Plant Cell Environ.* **41**, 1742-1748 (2018).
731   50.   de Montaigu, A., Tóth, R. & Coupland, G. Plant development goes like clockwork.
732   *Trends in Genetics* **26**, 296-306 (2010).
733   51.   Kolmos, E. *et al.* A Reduced-Function Allele Reveals That EARLY FLOWERING3
734   Repressive Action on the Circadian Clock Is Modulated by Phytochrome Signals in
735   Arabidopsis. *The Plant Cell* (2011).
736   52.   Dixon, L.E. *et al.* Temporal Repression of Core Circadian Genes Is Mediated through
737   EARLY FLOWERING 3 in Arabidopsis. *Curr. Biol.* **21**, 120-125 (2011).
738   53.   Kikis, E., Khanna, R. & Quail, P. ELF4 is a phytochrome-regulated component of a
739   negative feedback loop involving the central oscillator components CCA1 and LHY.
740   *Plant Journal* **44**, 300-313 (2005).
741   54.   Lu, S.X. *et al.* CCA1 and ELF3 Interact in the Control of Hypocotyl Length and
742   Flowering Time in Arabidopsis. **158**, 1079-1088 (2012).
743   55.   Huang, H. & Nusinow, D.A. Into the Evening: Complex Interactions in the Arabidopsis
744   Circadian Clock. *Trends in Genetics* **32**, 674-686 (2016).

745 56. Corbesier, L. *et al.* FT Protein Movement Contributes to Long-Distance Signaling in
746 Floral Induction of Arabidopsis. **316**, 1030-1033 (2007).
747 57. Jaeger, K.E. & Wigge, P.A. FT Protein Acts as a Long-Range Signal in Arabidopsis.
748 *Current Biology* **17**, 1050-1054 (2007).
749 58. Mathieu, J., Warthmann, N., Küttner, F. & Schmid, M. Export of FT Protein from
750 Phloem Companion Cells Is Sufficient for Floral Induction in Arabidopsis. *Current*
751 *Biology* **17**, 1055-1060 (2007).
752 59. Chen, X. *et al.* Shoot-to-Root Mobile Transcription Factor HY5 Coordinates Plant
753 Carbon and Nitrogen Acquisition. *Current Biology* **26**, 640-646 (2016).
754 60. Flis, A. *et al.* Defining the robust behaviour of the plant clock gene circuit with absolute
755 RNA timeseries and open infrastructure. *Open Biol* **5** (2015).
756 61. Salomé, P.A. & McClung, C.R. PSEUDO-RESPONSE REGULATOR 7 and 9 are
757 partially redundant genes essential for the temperature responsiveness of the
758 *Arabidopsis* circadian clock. *Plant Cell* **17**, 791-803 (2005).
759 62. Edwards, K.D. *et al.* Quantitative analysis of regulatory flexibility under changing
760 environmental conditions. *Mol. Syst. Biol.* **6** (2010).
761 63. Nakagawa, T. *et al.* Development of series of gateway binary vectors, pGWBs, for
762 realizing efficient construction of fusion genes for plant transformation. *J. Biosci.*
763 *Bioeng* **104**, 34-41 (2007).
764 64. Nakagawa, T. *et al.* Improved gateway binary vectors: high-performance vectors for
765 creation of fusion constructs in transgenic analysis of plants. *Biosci Biotechnol*
766 *Biochem.* **71**, 2095-2100 (2007).
767 65. Clough, S.J. & Bent, A.F. Floral dip: a simlified method for Agrobacterium-mediated
768 transformation of Arabidopsis thaliana. *Plant J.* **16**, 735-743 (1998).
769 66. Plautz, J.D. *et al.* Quantitative analysis of Drosophila period gene transcription in living
770 animals. *J. Biol. Rhythms* **12**, 204-217 (1997).
771 67. Czechowski, T., Stitt, M., Altmann, T., Udvardi, M.K. & Scheible, W.-R. Genome-
772 Wide Identification and Testing of Superior Reference Genes for Transcript
773 Normalization in Arabidopsis. *Plant Physiology* **139**, 5-17 (2005).
774 68. Dobin, A. *et al.* STAR: ultrafast universal RNA-seq aligner. *Bioinformatics* **29**, 15-21
775 (2013).
776 69. Liao, Y., Smyth, G.K. & Shi, W. featureCounts: an efficient general purpose program
777 for assigning sequence reads to genomic features. *Bioinformatics* **30**, 923-930 (2014).
778 70. Robinson, M.D., McCarthy, D.J. & Smyth, G.K. edgeR: a Bioconductor package for
779 differential expression analysis of digital gene expression data. *Bioinformatics* **26**, 139-
780 140 (2010).
781 71. Love, M.I., Huber, W. & Anders, S.J.G.B. Moderated estimation of fold change and
782 dispersion for RNA-seq data with DESeq2. *Genome Biol.* **15**, 550 (2014).
783 72. Tarazona, S., García-Alcalde, F., Dopazo, J., Ferrer, A. & Conesa, A. Differential
784 expression in RNA-seq: A matter of depth. *Genome Res.* **21**, 2213-2223 (2011).
785 73. Leng, N. *et al.* EBSeq: an empirical Bayes hierarchical model for inference in RNA-seq
786 experiments. *Bioinformatics* **29**, 1035-1043 (2013).
787 74. Robinson, J.T. *et al.* Integrative genomics viewer. *Nat. Biotech.* **29**, 24-26 (2011).
788 75. Thorvaldsdóttir, H., Robinson, J.T. & Mesirov, J.P. Integrative Genomics Viewer
789 (IGV): high-performance genomics data visualization and exploration. *Brief. Bioinform.*
790 **14**, 178-192 (2013).
791 76. Michael, T.P. *et al.* Network discovery pipeline elucidates conserved time-of-day-
792 specific cis-regulatory modules. *PLoS Genetics* **4**, e14 (2008).
793 77. Mockler, T. *et al.* The DIURNAL project: DIURNAL and circadian expression
794 profiling, model-based pattern matching, and promoter analysis. *Cold Spring Harb.*
795 *Symp. Quant. Biol.* **72**, 353-363 (2007).
796 78. Katari, M.S. *et al.* VirtualPlant: A software platform to support systems biology
797 research. *Plant Physiol.* **152**, 500-515 (2010).
798 79. Takens, F. Detecting strange attractors in turbulence. *Lecture Notes in Math* **898**, 366-
799 381 (1981).

800   80.   Stark, J. Delay embeddings for forced systems I. Deterministic forcing. *J. Nonlinear*
801   *Sci.* **9**, 255-332 (1999).
802   81.   Marwan, N., Romano, C.M., Thiel, M. & Kurths, J. Recurrence plots for the analysis of
803   complex systems. *Phys. Rep.* **438**, 237-329 (2007).
804   82.   Hirata, Y., Horai, S. & Aihara, K. Reproduction of distance matrices and original time
805   series from recurrence plots and their applications. *Eur. Phys. J. Spec. Top.* **164**, 13-22
806   (2008).
807   83.   Tanio, M., Hirata, Y. & Suzuki, H. Reconstruction of driving forces through recurrence
808   plots. *Phys. Lett. A* **373**, 2031-2040 (2009).
809   84.   Hirata, Y., Komuro, M., Horai, S. & Aihara, K. Faithfulness of Recurrence Plots: A
810   Mathematical Proof. *International Journal of Bifurcation and Chaos* **25**, 1550168
811   (2015).
812   85.   Khor, A. & Small, M. Examining k-nearest neighbour networks: Superfamily
813   phenomena and inversion. *Chaos (Woodbury, N.Y.)* **26**, 043101-043101 (2016).
814   86.   Small, M. *Applied Nonlinear Time Series Analysis: Applications in Physics, Physiology*
815   *and Finance*. (World Scientific, 2005).

816

831   **Author Contributions**

832   W.W.C, N.T. and J.R. performed the biological experiments. Y.H. performed the mathematical

833   analysis. S.P., S.J.D., D.A.N. and S.A.K. contributed with reagents and comments. P.M.

834   designed the experiments and wrote the manuscript. All authors read, revised, and approved the

835   manuscript.

836   **Competing interests**

837   The authors declare no competing interests.

838   **Additional information**

839   Extended data is available for this paper at XXX.

840   Supplementary information is available for this paper at XXX.

Figure Legends

843   **Fig. 1. Prevalent function of ELF4 sustaining circadian rhythms in roots. a,** Luminescence

844   of *CCA1::LUC* (*LUCIFERASE*) oscillation simultaneously measured in shoots (Sh)

845   (n=9) and roots (Rt) (n=9). Root luminescence signals are represented in the right Y-axis. **b**,

846   Period (left Y-axis) estimates of *CCA1::LUC* rhythms in shoots and roots (n=8 for each)

847   and amplitude (right Y-axis) estimates of *CCA1::LUC* rhythms in shoots (n=7) and

848   roots (n=8); data are represented as the median ± max and min; 25-75 percentile). *** p-

849   value<0.0001; two-tailed t-tests with 95% of confidence. **c**, Circadian time course

850   analyses of *CCA1* mRNA expression in WT Sh and Rt. **d**, Luminescence of

851   *CCA1::LUC* rhythms in WT (n=9) and *elf4-1* Rt (n=8). **e**, Luminescence of *LHY::LUC*

852   rhythms in WT (n=8) and ELF4-ox Rt (n=9). **f**, Circadian time course analyses of *PRR9*

853   mRNA expression in roots of WT and *elf4-1*. Sampling was performed under constant

854   light conditions (LL) following synchronization under light:dark cycles (LD). **a, c-f**,

855   Data are represented as the means + SEM. **g,** Heatmap of the median-normalized expression (Z-

856   scaled FPKM values) of DEGs following a hierarchical clustering using the Euclidean

857   distance. **h**, Relationship between average expression and fold change for each gene. **i**,

858   Volcano plot showing fold-change versus significance of the differential expression test.

859   Black dots represent genes that are not differentially expressed, while red and green dots

860   are the genes that are significantly up- and down-regulated, respectively. Circadian

861   phases of **j**, up- and **k**, down-regulated DEG in *elf4-1* roots. Radial axis represents the

862   subjective time (hours). White and gray areas represent subjective day and night,

863   respectively. The "n" values refer to independent samples. **a-k,** Data for all experiments

864   are representative of two biological replicates, with measurements taken from distinct

865   samples grown and processed at different times.

866

867   **Fig. 2. ELF4 moves from shoots to regulate rhythms in roots.** *CCA1::LUC* luminescence in

868   roots of ELF4-ox scion into **a**, *elf4-1* (n=4) and **b**, *elf4-2* (n=3) rootstocks. Water instead of

869   luciferin was added to the wells containing ELF4-ox shoots. *CCA1::LUC* luminescence in *elf4-*

870   *1* rootstocks with **c**, WT (n=8) and **d**, ELF4 Minigene (ELF4MG) (n=10) scions. WT scions do

871   not express reporters and water instead of luciferin was added to the wells containing ELF4MG

872   shoots. **a-d**, Schematic drawings depicting the different scion/rootstock combinations are shown

873   above each graph. **e**, Circadian time course analyses of *ELF4* mRNA expression in roots of WT,

874   *elf4-1* and ELF4-ox scion and *elf4-1* rootstocks. **f**, Luminescence of *LHY::LUC* rhythms in *elf4-*

875   *1* roots after injection in shoots of purified ELF4 (n=4) or GFP proteins (n=8) and *elf4-1* roots

876   as a control (n=6). **g,** Representative image showing the lack of fluorescence signals in roots of

877   WT scion and WT rootstock. **h,** Representative image showing fluorescence signals in roots of

878   ELF4-ox scion into *elf4-1* rootstock. Scale bar: 100 μm. **i,** Western-blot analysis of ELF4-GFP

879   protein accumulation (arrows) in roots of ELF4-ox-GFP scion (E4ox) grafted into *elf4-1*

880   rootstock (*e4-1*) (two pools of independent grafting assays, #1 and #2, are shown). Asterisks

881   denote non-specific bands. **j,** *CCA1::LUC* luminescence in *elf4-2* rootstocks grafted with

882   ELF4-x3GFP scions (n=5). Water instead of luciferin was added to the wells containing ELF4-

883   x3GFP shoots. **a-f, j,** Data are represented as the means + SEM. **k,** Protein features of various

884   plant mobile proteins. The "n" values refer to independent samples. **a-j,** Two biological

885   replicates were performed for all experiments, with measurements taken from distinct samples
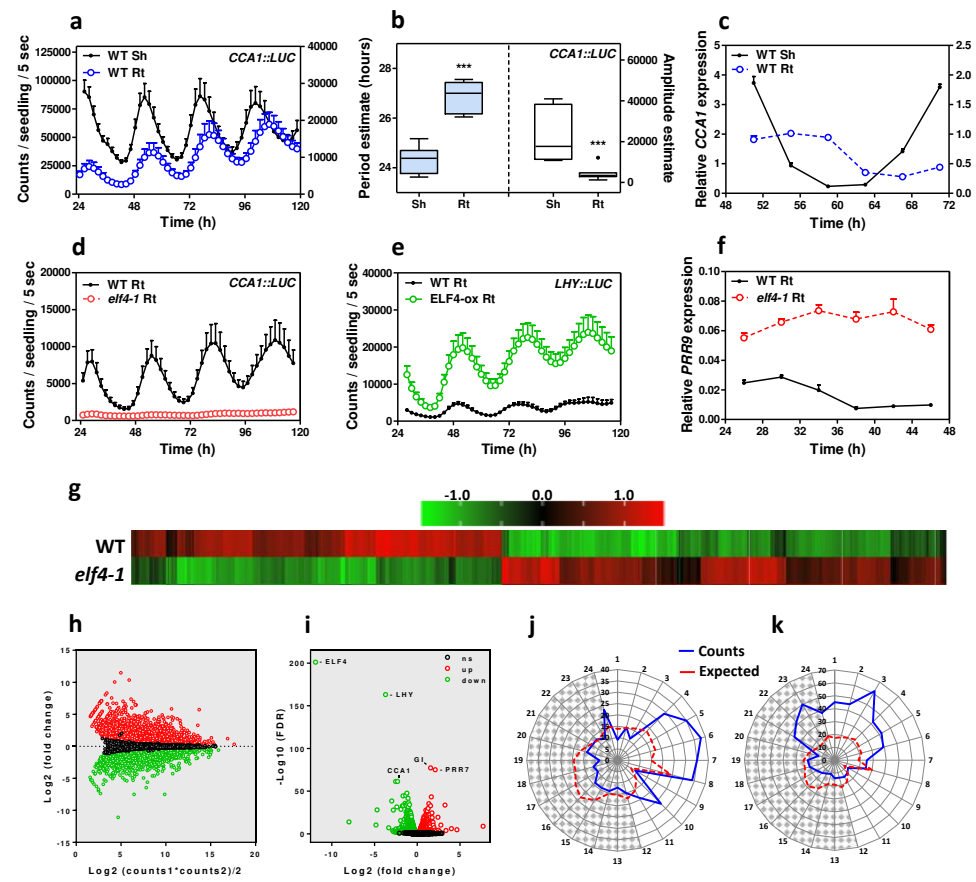
886   grown and processed at different times.

887

888   **Fig. 3. Mobile ELF4 does not regulate the photoperiodic-dependent phase in roots.**

889   Luminescence analyses of *PRR9::LUC* rhythms in **a**, roots (n=5 for ShD, n=6 for LgD) and **b**,

890   shoots (n=6 for ShD, n=4 for LgD) of plants grown under short day (ShD) or long day (LgD)

891   conditions. **c**, Western-blot analyses and **d**, quantification of ELF4 protein accumulation in

892   ELF4 Minigene roots (E4MG Rt) of plants grown under ShD and LgD (also in Extended Data

893   Fig. 8a-d). **e**, Western-blot analyses and **f**, quantification of ELF4 protein accumulation in

894   E4MG roots of plants grown under ShD and excised roots under LgD (also in Extended Data

895   Fig. 8a-f). Arrows indicate the ELF4 protein. Luminescence of *LHY::LUC* oscillation in WT,

896   ELF4-ox and *elf4-1* plants measured in **g**, shoots (Sh) (n=12) and **h**, roots (Rt) (n=12) under

897   LgD conditions. **a-b, d, f, g-h,** Data are represented as the means + SEM. Dashed lines indicate

898   dusk under LgD. The "n" values refer to independent samples. **a-h,** Two biological replicates

899   were performed for all experiments, with measurements taken from distinct samples grown and
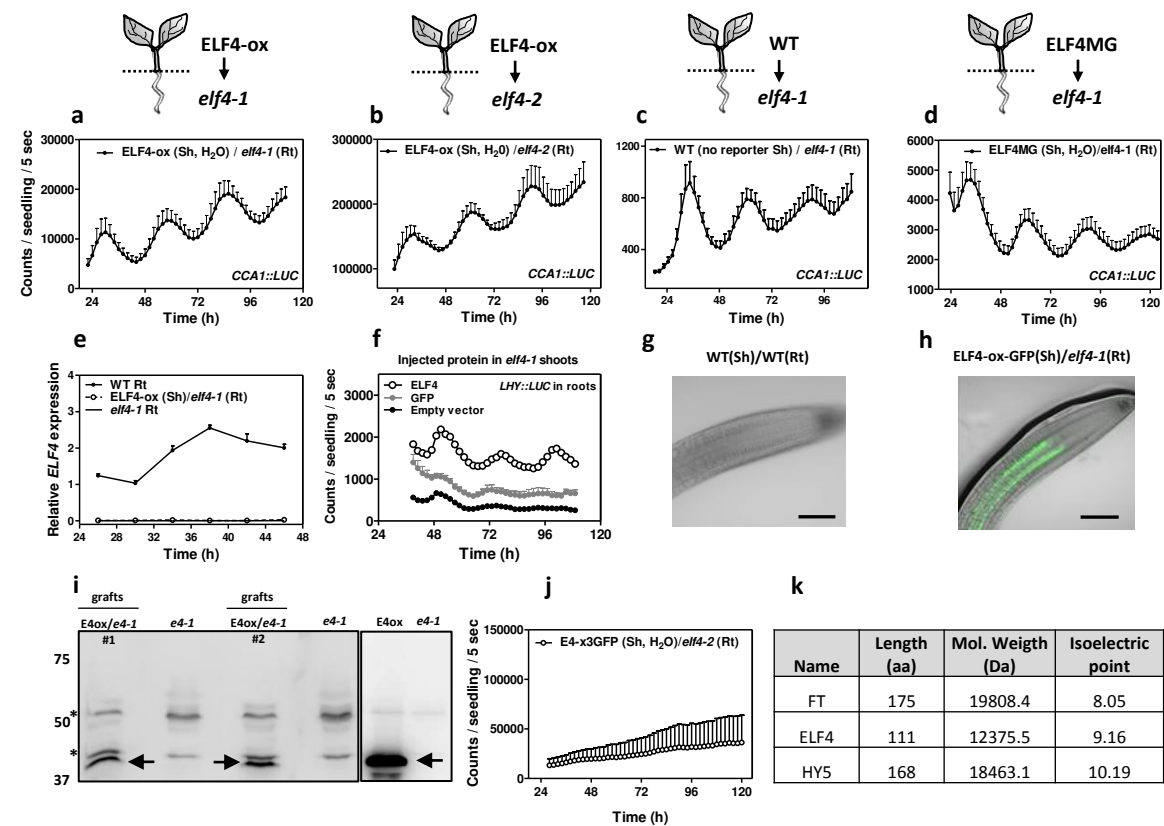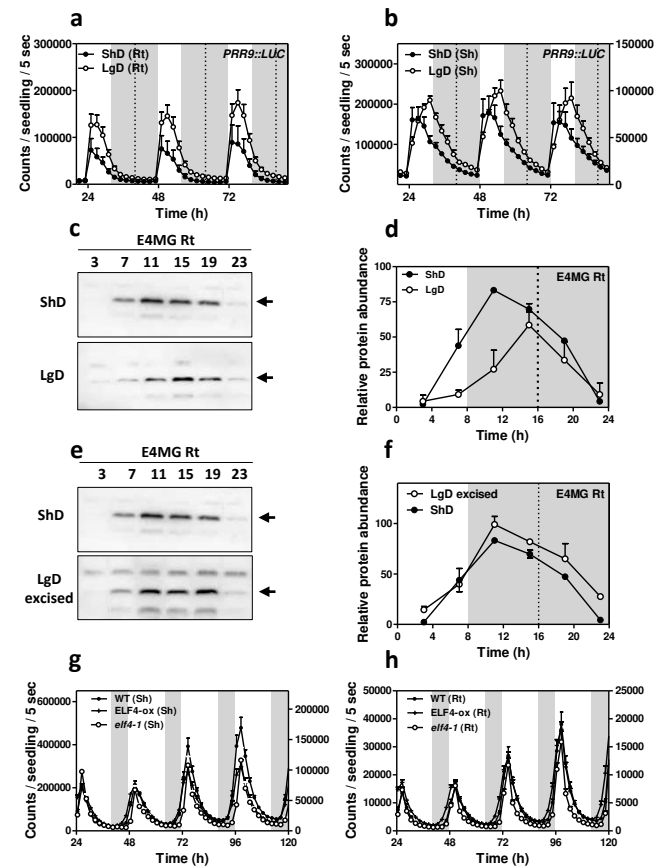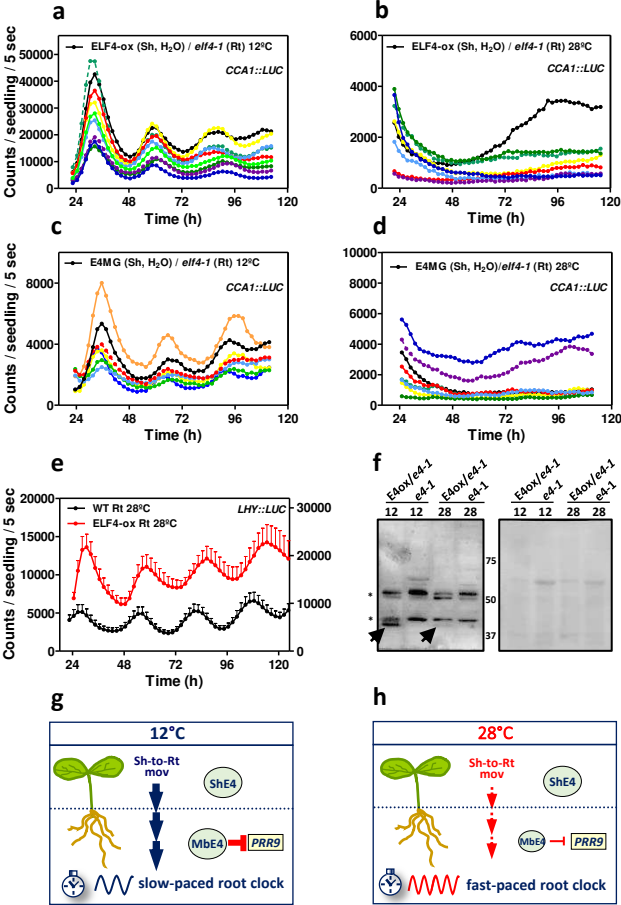
900   processed at different times.

901

902   **Fig. 4. Mobile ELF4 sets the temperature-dependent pace of the root clock.**

903   Individual luminescence waveforms of *CCA1::LUC* rhythmic oscillation in ELF4-ox scion into

904   *elf4-1* rootstocks at **a**, 12ºC (n=10) and **b**, 28ºC (n=8). Individual luminescence waveforms of

905   *CCA1::LUC* rhythmic oscillation in E4MG scion into *elf4-1* rootstocks at **c**, 12ºC (n=7) and **d,**

906   28ºC (n=8).Water instead of luciferin was added to the wells containing ELF4-ox and E4MG

907   scions. **e**, Luminescence of *LHY::LUC* rhythmic oscillation in WT and ELF4-ox roots at 28ºC

908   (n=8 for WT, n=5 for ELF4-ox). Data are represented as the means + SEM. **f**, Western-blot

909   analysis of ELF4-GFP protein accumulation (arrow) in roots of ELF4-ox-GFP scion (E4ox)

910   grafted into *elf4-1* rootstock (*e4-1*) at 12ºC and 28ºC. *elf4-1* mutant protein extracts were used

911   as a control. Asterisks denote non-specific bands. Ponceau S staining of the membrane is shown

912   in the right panel. Schematic drawing depicting **g**, the increased shoot-to-root movement of

913   ELF4 (Sh-to-Rt mov, thick blue vertical arrows), increased *PRR9* repression and the slow pace

914   of the root clock at low temperatures, and **h**, the decreased shoot-to-root movement (Sh-to-Rt

915   mov, thin red vertical arrows), decreased *PRR9* repression and fast-paced root clock at high

916   temperature. The "n" values refer to independent samples. **a-f,** Two biological replicates were

917   performed for all experiments, with measurements taken from distinct samples grown and

918   processed at different times.

Figure 1

Figure 2

a — ELF4-ox (Sh, H₂O) / *elf4-1* (Rt), *CCA1::LUC*, ELF-ox → *elf4-1*

b — ELF4-ox (Sh, H₂0) /*elf4-2* (Rt), *CCA1::LUC*, ELF-ox → *elf4-2*

c — WT (no reporter Sh) / *elf4-1* (Rt), *CCA1::LUC*, WT → *elf4-1*

d — ELF4MG (Sh, H₂O)/elf4-1 (Rt), *CCA1::LUC*, ELF4MG → *elf4-1*

e — Relative *ELF4* expression vs Time (h): WT Rt; ELF4-ox (Sh)/*elf4-1* (Rt); *elf4-1* Rt

f — Injected protein in *elf4-1* shoots, *LHY::LUC* in roots: ELF4, GFP, Empty vector

g — WT(Sh)/WT(Rt)

h — ELF4-ox-GFP(Sh)/*elf4-1*(Rt)

i — grafts: E4ox/*e4-1* #1, *e4-1*, E4ox/*e4-1* #2, *e4-1*, E4ox, *e4-1* (75, 50*, *, 37)

j — E4-x3GFP (Sh, H₂O)/*elf4-2* (Rt)

k

Name	Length (aa)	Mol. Weigth (Da)	Isoelectric point
FT	175	19808.4	8.05
ELF4	111	12375.5	9.16
HY5	168	18463.1	10.19

Figure 3

a

ELF4-ox (Sh, H₂O) / *elf4-1* (Rt) 12ºC

CCA1::LUC

Counts / seedling / 5 sec

Time (h)

b

ELF4-ox (Sh, H₂O) / *elf4-1* (Rt) 28ºC

CCA1::LUC

Time (h)

c

E4MG (Sh, H₂O) / *elf4-1* (Rt) 12ºC

CCA1::LUC

Counts / seedling / 5 sec

Time (h)

d

E4MG (Sh, H₂O)/*elf4-1* (Rt) 28ºC

CCA1::LUC

Time (h)

e

WT Rt 28ºC
ELF4-ox Rt 28ºC

LHY::LUC

Counts / seedling / 5 sec

Time (h)

f

g

12°C

h

28°C

a Shoots

WT(Sh)/WT(Rt)   *PRR9::LUC*

b Roots

WT Rt
WT(Sh)/WT(Rt)   *PRR9::LUC*

c

WT Sh
elf4-1 Sh
ELF4-ox Sh

d

ELF4-ox (Sh, H_2O) / *elf4-1* (Rt)

CCA1::LUC

e

elf4-2 Sh
elf4-2 Rt   *CCA1::LUC*

f

E4MG (Sh, H_2O)/*elf4-1* (Rt)

CCA1::LUC

a ELF4

1 2 3 4

ELF4 →

b GFP

1 2 3 4

← GFP

c

elf4-1

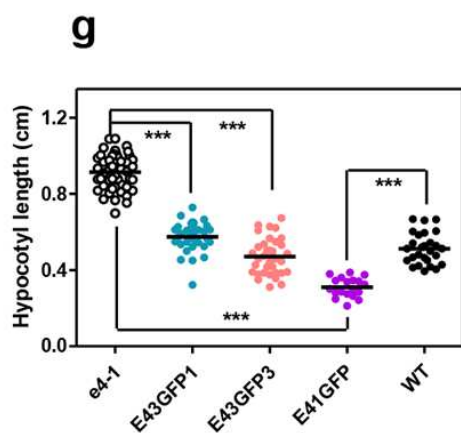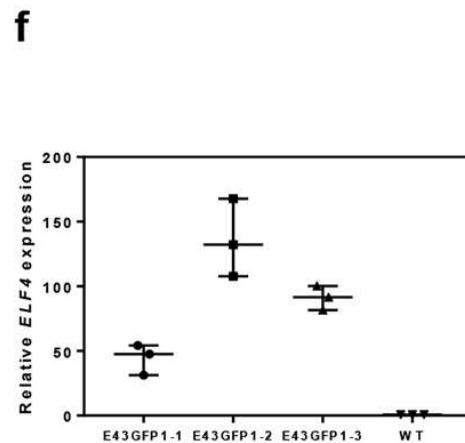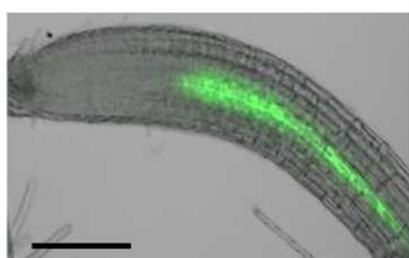ELF4 protein

d ELF4-ox-GFP(Sh)/*elf4-1*Rt)

e ELF4-ox-GFP(Sh)/*elf4-1*(Rt)

f

Relative *ELF4* expression

200
150
100
50
0

E43GFP1-1 E43GFP1-2 E43GFP1-3 WT

g

Hypocotyl length (cm)

1.2
0.8
0.4
0.0

e4-1 E43GFP1 E43GFP3 E41GFP WT

*** *** *** ***

h

Relative *ELF4* expression

6
4
2
0

75 79 83 87 91 95
Time (h)

● WT
○ E4-3xGFP

i

Relative *PRR9* expression

0.3
0.2
0.1
0.0

75 80 85 90 95
Time (h)

● WT
○ E4-3xGFP

j

Counts / seedling / 5 sec

150000
100000
50000
0

24 48 72 96 120
Time (h)

CCA1::LUC

● WT(Sh H₂O)/WT(Rt)
○ *elf4-1*(Sh H₂O)/*elf4-1*(Rt)

k

Counts / seedling / 5 sec

15000
12000
9000
6000
3000
0

24 48 72 96 120
Time (h)

CCA1::LUC

○ *elf4-1*(Sh H₂O)/*elf4-1*(Rt)

a

b

c

d

e

f

g

h

i

j

k *PRR9*

WT int

WT exc

l

Intact *elf4-1* Rt

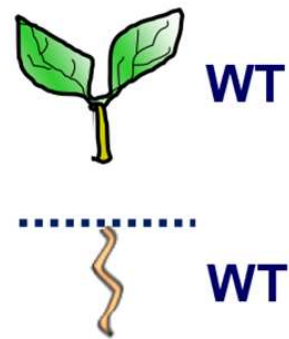Excised WT Rt

elf4-1

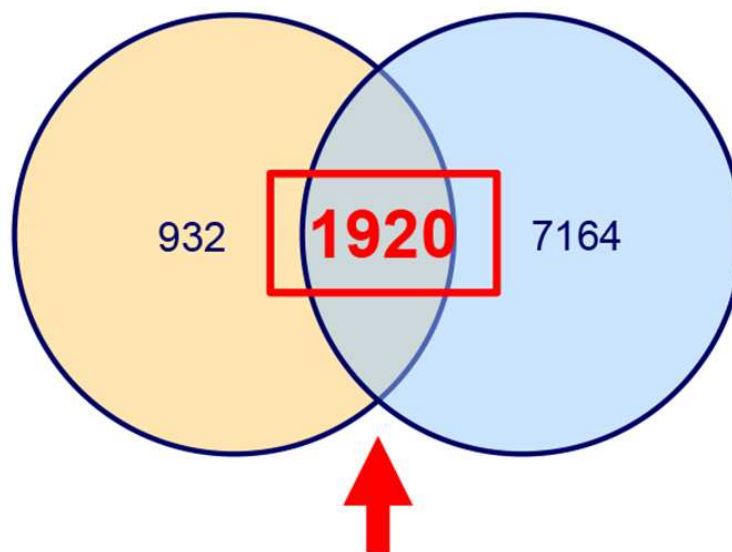*elf4-1*

WT

WT

elf4-1 intact   WT excised

932   **1920**   7164

67,32% of the DEGs in *elf4-1* intact roots are also differentially regulated in WT excised roots. The overlapped DEGs are not affected by excision as *elf4-1* mutant roots are intact.

a

E4MG Rt

3 7 11 15 19 23

ShD ←

ShD
excised ←

b

Relative protein accumulation

○ ShD excised
● ShD

E4MG Rt

Time (h)

c

E4MG Rt

3 7 11 15 19 23

LgD ←

LgD
excised ←

d

Relative protein accumulation

○ LgD excised
● LgD

E4MG Rt

Time (h)

e

E4MG Rt

3 7 11 15 19 23

ShD
excised ←

LgD
excised ←

f

Relative protein abundance

○ LgD excised
● ShD excised

E4MG Rt

Time (h)